Superalloys 2008
Roger C. Reed, Kenneth A. Green, Pierre Caron, Timothy P. Gabb, Michael G. Fahrmann, Eric S. Huron and Shiela A. Woodard
TMS (The Minerals, Metals & Materials Society), 2008

AN INVESTIGATION OF THE COMPATIBILITY OF NICKEL-BASED SINGLE CRYSTAL SUPERALLOYS WITH THERMAL BARRIER COATING SYSTEMS

R.T. WU[1], K. KAWAGISHI[2], H. HARADA[2] AND R.C. REED[3]
[1]Dept of Materials, Imperial College London, Prince Consort Road; London, SW7 2BP, UK
[2]National Institute for Materials Science, 1-2-1 Sengen, Tsukuba City, Ibaraki, JAPAN
[3]Dept of Metallurgy & Materials, University of Birmingham; Edgbaston, B15 2TT, UK

Keywords: thermal barrier coatings, compatibility of, spallation life, spallation mechanism

Abstract

The compatibility of a number of nickel-based single crystal superalloys with a thermal barrier coating (TBC) system is examined. An industry-standard yttria-stabilised zirconia (YSZ)-type ceramic was used throughout this work, deposited using electron beam physical vapour deposition at a commercial facility. It is demonstrated that the resistance to spallation during thermal cycling is dependent upon the composition of the superalloy substrate upon which the TBC system is placed – the number of cycles to failure is found to vary by up to a factor of three when identical TBC systems (bond coat, ceramic layer) are employed. Of the three different bond coat systems considered, a platinum-diffused (so-called low-cost bond coat) was found to be consistently better than both low-activity or high-activity platinum aluminide bond coats, but only marginally. The composition of the superalloy substrate is thus shown to be the primary factor in determining TBC life.

Introduction

Single crystal (SC) superalloys [1] have traditionally been designed with the priority to optimise the creep, fatigue, oxidation and corrosion-resistant properties. However, as the demand for better fuel efficient tubine systems continues, it is required that the substrate materials must now be coated with thermal barrier coatings (TBCs) [2,3] to enhance the high temperature capability of critical turbine components such as turbine blades and guide vanes. Yet, it is known that TBC coated nickel-base superalloys are prone to spallation [4]; for this reason, several bond coat technologies have been developed as a mean to enhance the mutual compatibility of the two by improving the oxidation resistance of the coated specimens.

Unfortunately, little work [5,6] has been reported to elucidate the compatibility issues of superalloys with the TBCs. More importantly, the influence of the substrate composition on the TBC spallation life is little studied and not well understood. This is despite much progress which has been made to emphasise the micromechanics of the failure mode of TBCs [7,8]. In particular, the approach in modeling TBC failure [9-13] generally relies on the treatment of the oxidation-induced stresses that drive TBC spallation despite the fact that it might reasonably be assumed that the TBC life and the modes of failure (i.e. location of interfacial failure) are also influenced significantly by the inherited chemistry of the underlying superalloys.

In this study, the compatibility of a number of nickel-based single crystal superalloy with thermal barrier coating systems has been investigated. It has been demonstrated conclusively that the compositions of these alloys play an important part in determining the TBC's spallation resistance.

Experimental Details

Fully heat-treated (solution and primary-aged) single crystal alloys of SRR99, CMSX-4, TMS-82+, PWA-1484 and TMS-138A processed using conventional investment casting methods into cylindrical rods (10 mm in diameter) were used as substrate materials for this research. The chemical compositions of the alloys considered are given in Table 1. The five alloy rods were cut to disc-shape (10 mm diameter and 4mm thickness), spot welded onto rectangular Nimonic 80A sticks. Three commercial bond coat systems, a high temperature low activity Pt-Al (CN91PA) one, a low temperature high activity Pt-Al (so-called RT22LT) one and a Pt diffusion (so-called low-cost) bond coat, were subsequently deposited onto the flat surfaces of the button-shaped discs.

The high temperature low activity Pt-Al bond coat and the low temperature high activity Pt-Al bond coat specimens were electrodeposited with a thin layer of platinum of 5 and 7 μm respectively, followed by a vacuum heat treatment applied at 1100°C for 1 hour. Then, 5 hr vapour phase and 20 hr pack-aluminisation processes were applied respectively. The Pt-diffusion bond coat specimen was electrodeposited with a 10 μm platinum layer and was vacuum heat treated at 1150°C for 1 hour subsequently. It should be emphasised that no aluminisation process was applied. All specimens were further heat-treated for 1 hour at 1100°C in argon atmosphere and a ZrO_2 /7wt% Y_2O_3 (175μm thickness) was then deposited by the electron beam - physical vapour deposition (EB-PVD) method. A further vacuum heat treatment (1100°C, 1 hr) and aging (870°C, 16 hrs) were applied. These coatings were applied consistent with commercial practice by Chromalloy UK Ltd.

The TBC coated specimens were then subjected to thermal cyclic oxidation testing in a purpose-built rig (See **Figure 1**). The thermal profile of 1 hour heating to furnace temperature of 1135°C and 1 hour fan-assisted cooling by laboratory air was used. For analysis after thermal cycling, microstructure imaging was carried out in a field emission gun scanning electron microscope (FEGSEM). Quantitative chemical analysis was done by field emission - electron proble micro-analysis (FE-EPMA) equipped with wavelength dispersive X-ray (WDX) system. Five individual specimens of each TBC system were used to determine the average TBC spallation lifetime, to evaluate the scatter in the experimental results.

Table 1. Nominal chemical composition, wt%, of the nickel-based superalloys considered.

Element	Co	Cr	Mo	W	Al	Ti	Ta	Hf	Re	Ru	C	Ni
SRR99	5.0	8.0	-	9.5	5.5	2.2	2.8	-	-	-	0.011	Bal.
TMS-82+	7.8	4.9	1.9	8.7	5.3	0.5	6.0	0.1	2.4	-	-	Bal.
PWA1484	10.0	5.0	2.0	6.0	5.6	-	8.7	0.1	3.0	-	-	Bal.
CMSX-4	9.6	6.5	0.6	6.4	5.6	1.0	6.5	0.1	3.0	-	-	Bal.
TMS-138A	5.8	3.2	2.8	5.6	5.7	-	5.6	0.1	5.8	3.6	-	Bal.

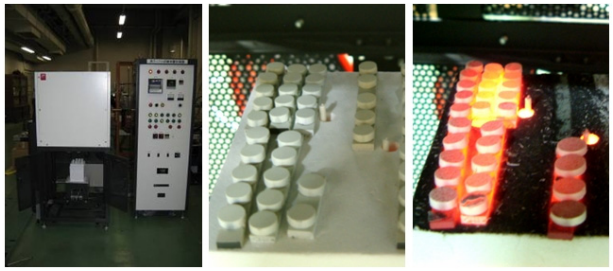

Figure 1. Pictures showing the use of the thermal cycling furnace (left), the placement of specimens on the sample stage (centre) and the heating/cooling conditions (right).

Results

Characterisation of Coating Cross-Sections – As Received Condition

Scanning electron micrographs representing the typical microstructures of the three coatings on a CMSX-4 substrate in the as-received condition are given in **Figure 2**.

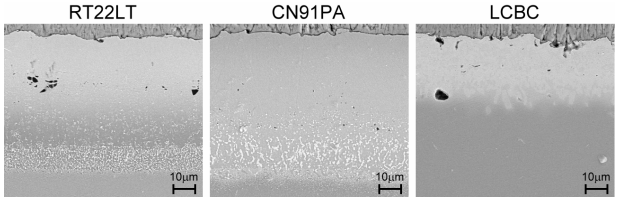

Figure 2. The microstructures of the coatings (RT22LT, CN91PA, and LCBC) in the as-received condition.

The microstructures of Pt-diffusion coatings on CMSX-4 substrates are also shown in **Figure 3**. In all cases, the TBC layers have been prepared to similar thickness. It can be seen that the only differences are between the microstructures and the thicknesses of the bond coats. Pt-Al bond coat systems produce a single phase microstructure of β-NiAl with Pt in solid solution (i.e. (Pt, Ni)Al). Below the grit-line of residual Al_2O_3 particles from the grit blasting process is the inner multi-phase layer of the coating consisting of precipitates rich in refractory metals (Ta, W, Mo) in the β phase matrix. The Pt-diffusion bond coat consists of a two phase γ and γ' microstructure both above and below the grit-line; the β-NiAl phase is completely absent since the aluminisation process is not performed. Al and Pt EDX concentration line-profiles of these coatings are shown in **Figure 4**. In all cases, the post-processing heat treatment has resulted in the formation of a very thin thermally-grown oxide (TGO) layer even prior to any thermal cycling taking place.

Thermal Cyclic Oxidation Testing

Based on the results of the thermal cycling experiment, it was found that coating life varied significantly with the composition of the superalloy substrate as illustrated in **Figure 5**. For instance, TBC coated PWA1484 exhibited spallation lifetimes at least three times superior to those of first generation superalloy SRR99 regardless of the types of bond coat being applied, suggesting that strong chemical effects were inherited from the substrate. In addition, the spallation resistance of TBC coated 4th generation TMS-138A behaved significantly better than that of SRR99 and comparable to that the second generation superalloy CMSX-4, suggesting that no detrimental effect is inherited from ruthenium addition to the substrate. It should be noted here that the thermal exposure of PWA-1484 specimens coated with Pt-diffusion bond coat was interrupted at the 1000th cycle as the purpose of demonstrating TBC spallation resistance had been fulfilled. These findings confirm a composition-dependence of the TBC spallation life, and can be explained only by the different degradation mechanisms taking place in the bond coat or near the TGO interfaces (since the bond coat and the ceramic top coat were prepared to be identical).

In term of the bond coat technology, it was demonstrated in general that the type of bond coat being applied had less influence on the TBC spallation life than the substrate effect. It was shown as well that platinum-diffusion LCBC bond coats outperformed both platinum aluminide systems.

Mechanism of TBC Failure

As previously demonstrated, the composition of the superalloy substrates has a first order influence on the TBC spallation life than that of the bond coat materials. For this reason, attention is focused in this section on the study the substrate effect on the mechanism of TBC failure, at a fixed TBC condition. Pt-diffuson LCBC bond coat was chosen for this investigation as it best amplified the substrate effect on the coating spallation life.

SEM images of the fracture interface for each of the five substrates are shown in **Figure 6**. It has been found that decohesion occurred at an interface position which depended on the substrate composition. In particular, it has also been observed that specimens with shorter TBC spallation life tended to fail at the TGO / bond coat interface; while more spallation-resistant coatings failed within the TGO. In addition, based on these electron images, the thickness of the TGO at failure for each of the specimens was measured and plotted along with the TBC life for comparison as illustrated in **Figure 7**.

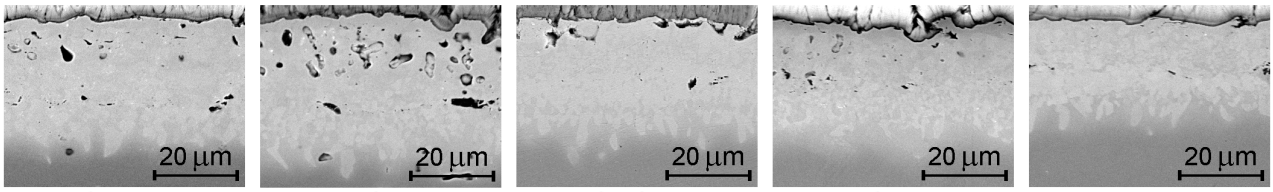

Figure 3. The microstructures of Pt-diffusion coatings on the superalloy substrates.

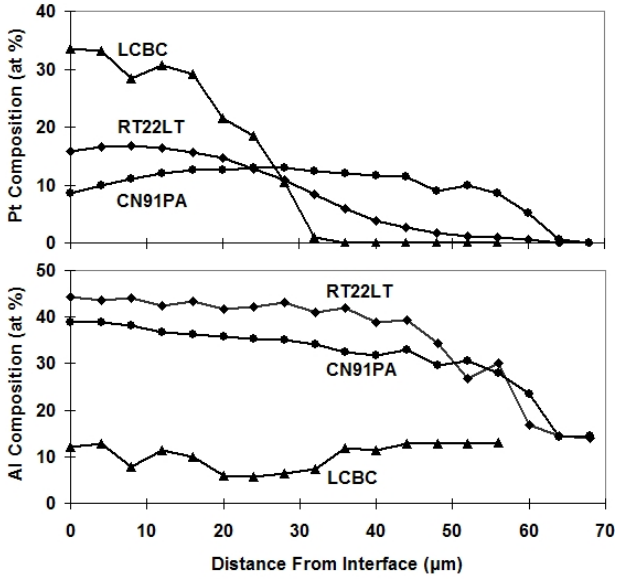

Figure 4. EDX concentration line-profile of Pt and Al in the bond coat for the as-received RT22LT, CN91PA and LCBC specimens.

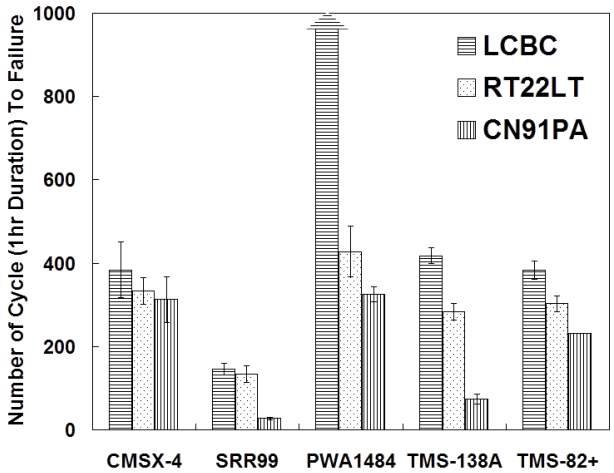

Figure 6. TBC spallation life for cyclic oxidation testing (1 hour thermal cycling condition) of TBC coated superalloys.

Based on these results, it can be seen that the TGO thickness at failure in TMS-138A is considerably thicker than that of the TMS-82+, even though TBC coated TMS-138A offered slightly longer TBC spallation life than TMS-82+. Moreover, despite the

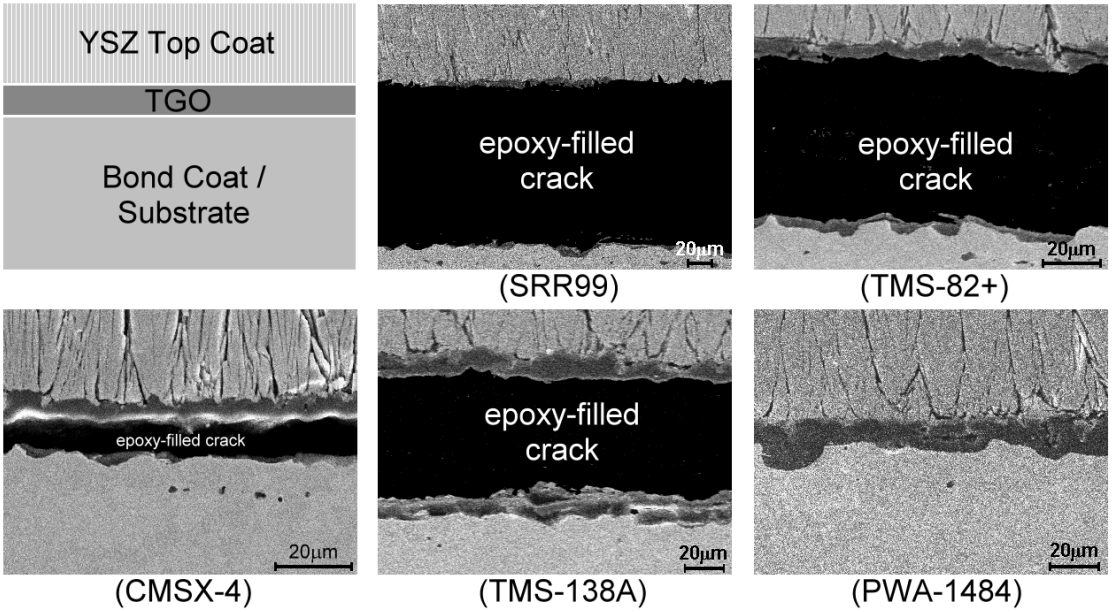

Figure 5. SEM micrographs illustrating the location of interfacial spallation failure of TBC (LCBC) coated superalloys.

Table 2. Elemental compositions (wt%) of the TGO layers measured by WDS FE-EPMA analysis

Element	Pt	Zr	Y	Co	Re	Ta	Mo	Al	Ni	Ru	W	Ti	Cr	O
SRR99	0.3	0.8	0.1	0.1	-	0.0	-	51.6	0.5	-	0.1	0.0	0.2	46.2
TMS-82+	0.5	0.7	0.1	0.1	0.1	0.1	0.0	51.6	0.6	-	0.1	0.0	0.1	45.9
PWA1484	0.5	0.9	0.1	0.1	0.1	0.1	0.0	51.6	0.7	-	0.1	-	0.1	45.6
CMSX-4	0.3	0.9	0.1	0.1	0.1	0.1	0.0	48.8	0.7	-	0.0	0.0	0.1	48.7
TMS-138A	0.4	0.8	0.1	0.1	0.1	0.0	0.0	51.7	0.6	0.0	0.1	-	0.0	46.0

fact that the TBC lifetimes of CMSX-4, TMS-138A and TMS-82+ were within a few cycles to each other, their TGO growth kinetics are very different, under the assumption of a parabolic growth-rate type. Thus, it seems that there is little correlation between the oxide growth kinetics and the TBC spallation life.

High Resolution Analysis and Mapping by EPMA/WDX

Elemental compositions of the TGO layers on the three bond coats were characterized using WDS analysis, see Table 2. The results are quoted only for specimens with elemental TGO thickness greater than the spatial resolution of the FE-EPMA/WDX technique. Chemical mapping of the bond coat near the TGO interfaces was also carried out to determine the elemental chemical distributions on specimens after 100-cycle thermal exposure as shown in Figures 8-12. Both results suggest that among all specimens, the oxide layers are primarily of Al_2O_3. However, it has also been observed for some specimens that either islands or continuous layers of Ni, Cr and, or Co –rich oxides are present above the primarily Al_2O_3 layer. For example, CMSX-4, TMS82+, TMS-138A and PWA1484 all contain islands which are rich in Cr; while TMS82+, TMS138A and PWA1484 further contain islands rich in Ni. In addition, presence of Co rich regions has also been noticed on TMS-82+ and TMS-138A. For SRR99 specimens, fairly continuous Ni, Cr and Co –rich oxides have been confirmed. However, it should be recognised that the amount of spinel phases in the TGO is very small in any of the TBC coated systems; the TGO thickness upon failure varies between different alloys is essentially a measure of the amount of alumina.

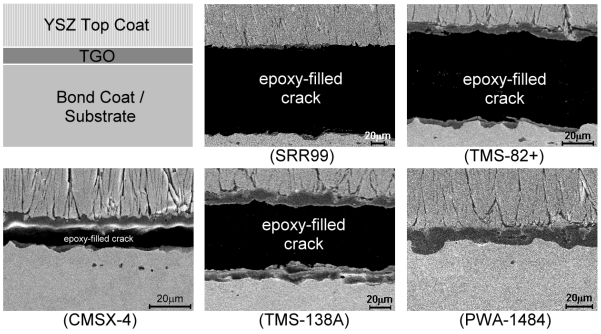

Figure 7. SEM micrographs illustrating the location of interfacial spallation failure of TBC (LCBC) coated superalloys.

Discussion

The results presented here provide new insights into the current understanding of thermal barrier coating systems (TBCs). Traditionally, one considers that TBC spallation occurs as the stored elastic energy of the coating, which stiffens with time due to sintering, exceeds the interfacial adhesion between the TGO

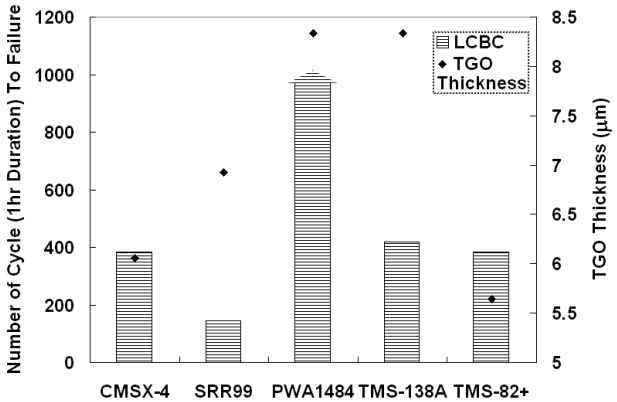

Figure 8. TBC spallation life vs the thickness of TGO upon failure; illustrating no clear correlation between the two.

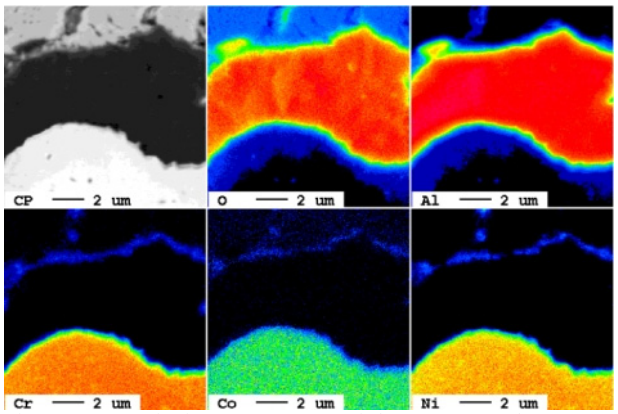

Figure 9. Quantitative WDX maps of the TBC coated SRR99 - LCBC system following 100 cycle exposure at 1135°C.

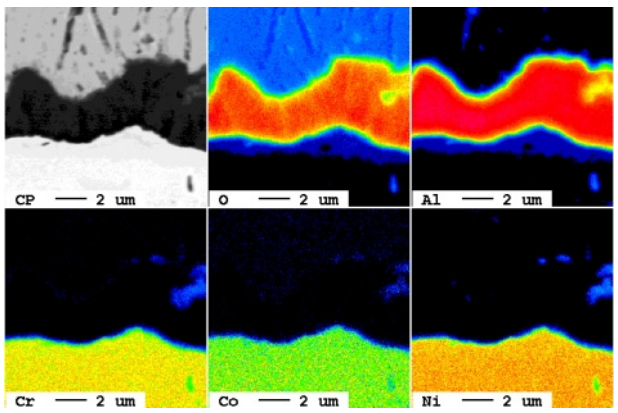

Figure 10. Quantitative WDX maps of the TBC coated TMS-82+ - LCBC system following 100 cycle exposure at 1135°C.

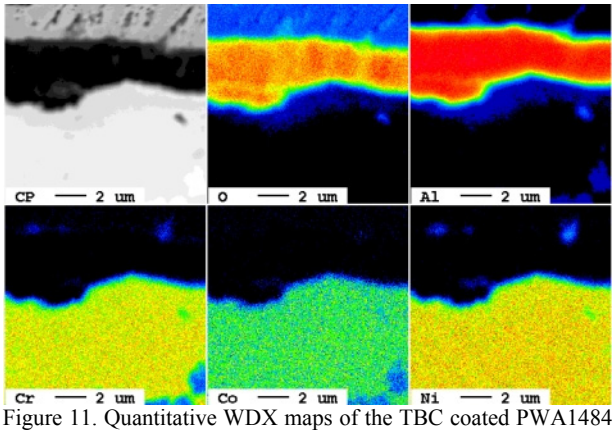

Figure 11. Quantitative WDX maps of the TBC coated PWA1484 - LCBC system following 100 cycle exposure at 1135°C.

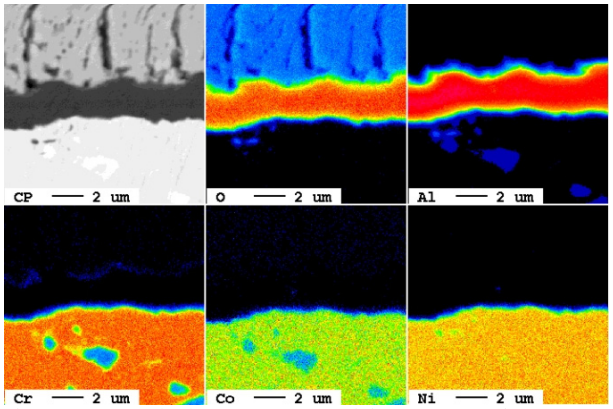

Figure 12. Quantitative WDX maps of the TBC coated CMSX-4 - LCBC system following 100 cycle exposure at 1135°C.

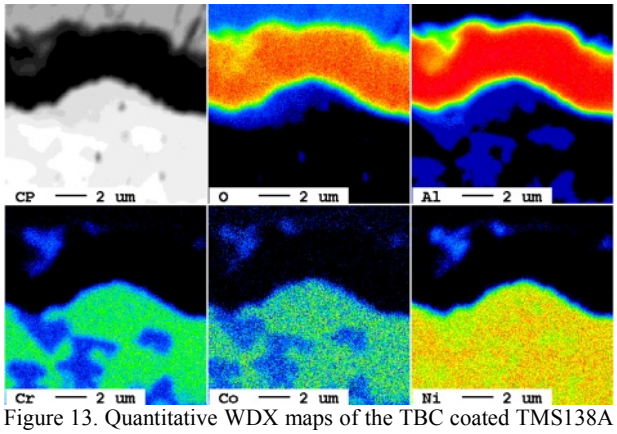

Figure 13. Quantitative WDX maps of the TBC coated TMS138A - LCBC system following 100 cycle exposure at 1135°C.

and bond coat. In addition, studies [14, 15] have shown that in the situation for a thin film of thickness h on a thick substrate and the case of edge delamination, a driving force G exists for TBC spallation as

$$G = \frac{1}{2}\left(\frac{1-\nu^2}{E}\right)\sigma_0^2\, h$$

where E and ν are the elastic modulus and Poisson's ratio of the film respectively and σ_o the compressive misfit stress. Associating h with the TGO and the σ_o as the residual compressive stress in the TGO, the generalised argument is that the driving force for spallation (G) increases as the TGO thickens and the misfit stress in the TGO develops; delamination occurs when G reaches the critical interfacial fracture toughness G_c.

However, the current findings have conclusively confirmed that the resistance of TBC to spallation during thermal cycling is strongly dependent upon the composition of the superalloy substrate upon which the TBC system is placed. In particular, as the EPMA mapping has revealed, due to some minor segregation of Ni, Cr and Co above the Al_2O_3 TGO layer, a time-dependent diffusion process driven by the oxidation, may likely degrade the adhesion of the coating. In addition, the presence of Ti as an alloying element in SRR99, TMS-82+, CMSX-4 may also impact the TBC life. In fact, previous studies of ours [16] and others [17, 18] have suggested that fast diffusion of Co and Ti to the surface leads to the formation of cobalt and titanium rich oxides, causing an increase in the rates of oxidation. In addition, Ti^{4+} ions, reported [19] to substitute for Al^{3+} ones to create aluminium vacancies within the scale may also enhance the rate of oxide-scale growth. Thus, it is not difficult to explain the reason why SRR99, among the alloys considered, exhibits the fastest oxidation rate and the shortest TBC life. Regarding the spallation mechanisms as mentioned previously, it appears that specimens with shorter TBC spallation life preferentially failed at the TGO / bond coat interface; while more spallation-resistant coatings failed with the TGO.

This leads to a proposed argument that the interfacial adhesive strength of TBCs, which controls the TBC lifetime, is a dynamic materials property dependent on and influenced considerably by the composition of the substrate materials (i.e. superalloys). This situation can be qualitatively represented by a schematic drawing (**Figure 13**) which illustrates the variation of the driving force G and the interfacial fracture toughness Gc with the time of thermal exposure.

Based upon the first order approximation that the driving force G will increase linearly with TGO thickness and hence parabolically with time t as shown, then thermal cycling at higher temperatures will accelerate the kinetics. The variation of Gc is also shown. At the beginning, for any choice of bond coat, Gc can be considered roughly uniform for all alloy systems consistent with the identical processing conditions employed. However, upon thermal exposure as the harmful elements diffuse to the TGO interface, the value of Gc decreases – rapidly for a substrate system such as the SRR99 and modestly for PWA1484 with other alloys of consideration falling somewhere between the two.

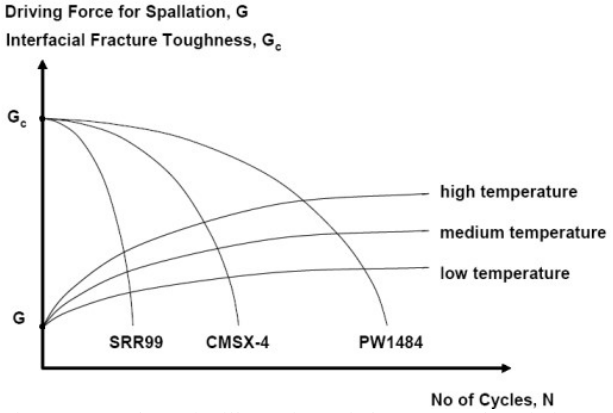

Figure 14. Schematic illustration of the proposed variation of driving force G and interfacial fracture toughness Gc during thermal cycling.

It should be recognised that studies published so far have tended to consider just a single substrate composition with a TBC placed upon it; thus, any influence of the substrate chemistry is then factored out from the experiment. It would appear that the superalloy composition has a first-order influence on the lifetime of the systems due to the sensitivity of the interfacial fracture toughness to substitutional elements diffusing through the bond coat system from the superalloy substrate beneath it. Our findings have implications for the design of TBC systems for the protection of the turbine blade aerofoils used for high temperature applications. Traditionally, nickel-base single crystal superalloys have been designed with their mechanical properties – particularly in creep and fatigue – in mind. However, as the operating conditions of modern gas turbines continue to become more aggressive and thermal barrier coatings (TBCs) for the provision of thermal insulation are being used increasingly, further property of the superalloy substrate is then required: that of compatibility with the TBC which it is required to support. In particular, the influence of different alloying elements present in the superalloy on the TBC's interfacial fracture toughness needs to be better understood.

Conclusions

The following conclusions can be drawn from this work:

1. It is demonstrated conclusively that the compatibility of modern nickel-based single crystal superalloys with thermal barrier coating (TBC) systems depends acutely upon their chemical composition.

2. In the tests reported here, TBC spallation life was found to vary by a factor of up to three, depending upon the chemical composition of the superalloy substrate; this effect implies that considerable chemical effects are at play.

3. By comparison, the details of the bond coat employed do not influence life so strongly.

4. An improvement of about 10% in spallation life was nonetheless displayed by the so-called low-cost bond coat system. This was observed consistently for the different substrate compositions considered.

5. These results can be explained only if the fracture toughness parameters controlling decohesion – for example the fracture toughness of the thermally grown oxide (TGO) and the fracture toughnesses of the interfaces bounding it – are influenced strongly by small changes in composition arising from interdiffusion with the bond coat, which itself inherits elemental changes from the substrate.

6. Single crystal superalloys have traditionally been designed with mechanical performance in creep and fatigue in mind. The results reported here demonstrate that a further factor has now emerged: compatibility with the thermal barrier coating systems placed upon them.

7. For optimum turbine blade aerofoil characteristics in service, it may now be necessary to sacrifice some of the mechanical behaviour of the substrate in order to improve the performance of the system as a whole.

Acknowledgements

Two of the authors (RW and RCR) acknowledge a grant from the EPSRC (EP/D04619X/1) which has been used to fund this work.

References

1. R.C. Reed, "Superalloys: Fundamentals and Applications", Cambridge University Press, (2006).

2. C.G. Levi, "Emerging materials and processes for thermal barrier systems", Current Opinion in Solid State and Materials Science, 8 (2004), 77-91.

3. N.P. Padture, M. Gell and E.H. Jordan, "Thermal barrier coatings for gas-turbine applications", Science, 296 (2002), 280-284.

4. V.K. Tolpygo and D.R. Clarke, "On the rumpling mechanism in nickel-aluminide coatings, part I: an experimental assessment", Acta materialia, 52 (2004), 5115-5127.

5. B.A. Pint, I.G. Wright, W.Y. Lee, Y. Zhang, K. Prussner and K.B. Alexander, "Substrate and bond coat compositions: factors affeccting alumina scale adhesion", Materials Science and Engineering, A245 (1998), 201-211.

6. B.A. Pint, "The role of chemical composition on the oxidation performance of aluminide coatings", Surface and Coatings Technology, 188-189 (2004), 71-78.

7. B.A. Pint, I.G. Wright, W.Y. Lee, Y. Zhang, K. Prussner and K.B. Alexander, "Substrate and bond coat compositions: factors affeccting alumina scale adhesion", Materials Science and Engineering, A245 (1998), 201- 211.

8. B.A. Pint, J.A. Haynes, K.L. More and I.G. Wright, "The use of model alloys to understand and improve the performance of Pt-modified aluminide coatings", Superalloys 2004, edited K.A. Green, T.M. Pollock, H. Harada, T.E. Howson, R.C. Reed, J.J. Schirra and S. Walston, (Warrendale, PA, USA: The Minerals, Metals and Materials Society (TMS), 2004), 597-606.

9. E. P. Busso, J. Lin and S. Sakurai, “A mechanistic study of oxidation-induced degradation in a plasma-sprayed thermal barrier coating system: Part II: Life prediction model”, Acta Materialia, Volume 49, Issue 9, 25 May 2001, 1529-1536.

10. F. Traeger, M. Ahrens, R. Va[ss]en and D. Stover, “A life time model for ceramic thermal barrier coatings”, Materials Science and Engineering A, Volume 358, Issues 1-2, 15 October 2003, 255-265.

11. E.P. Busso, L. Wright, H.E. Evans, L.N. McCartney, S.R.J. Saunders, S. Osgerby and J. Nunn, “A physics-based life prediction methodology for thermal barrier coating systems”, Acta Materialia, Volume 55, Issue 5, March 2007, 1491-1503.

12. M. Baker, J. Rosler and G. Heinze, “A parametric study of the stress state of thermal barrier coatings Part II: cooling stresses”, Acta Materialia, Volume 53, Issue 2, 10 January 2005, 469-476.

13. M. Jinnestrand and S. Sjostrom, “Investigation by 3D FE simulations of delamination crack initiation in TBC caused by alumina growth”, Surface and Coatings Technology, Volume 135, Issues 2-3, 15 January 2001, 188-195.

14. S.R. Choi, J.W. Hutchinson and A.G. Evans, “Delamination of multilayer thermal barrier coatings”, Mechanics of Materials, 31 (1999), 431-447.

15. M.Y. He, D.R. Mumm and A.G. Evans, “Criteria for the delamination of thermal barrier coatings; with application to thermal gradients”, Surface and Coatings Technology 185 (2004), 184-193

16. R.T. Wu and R.C. Reed, “On the compatibility of single crystal superalloys with a thermal barrier coating system”, Acta Materialia 56, Issue 3, February 2008, 313-323.

17. 40. B. A. Pint, J. A. Haynes, K. L. More, I. G. Wright, C. Leyens, “Compositional effects on aluminide oxidation performance: objectives for improved bond coats”, Superalloys 2000, edited T.M. Pollock, R.D. Kissinger, R.R. Bowman, K.A. Green, M. McLean, S.L. Olson and J.J. Schirra, (Warrendale, PA, USA: The Minerals, Metals and Materials Society (TMS), 2000), 629–638.

18. Andrew L. Purvis and Bruce M. Warnes, “The effects of platinum concentration on the oxidation resistance of superalloys coated with single-phase platinum aluminide”, Surface and Coatings Technology 146-147, September-October 2001, 1-6.

19. P. Fox, G.J. Tatlock, “Effect of tantalum additions on oxidation of overlay coated superalloys”, Materials Science and Tecchnology. 5 (1989) 816.